TWO-DIMENSIONAL MODELING OF EWT MULTICRYSTALLINE SILICON SOLAR CELLS AND COMPARISON WITH THE IBC SOLAR CELL

Mohamed M. Hilali, Peter Hacke, and James M. Gee
Advent Solar, Inc.
800 Bradbury Drive S.E, Suite 100, Albuquerque, NM 87106

ABSTRACT

In this study two-dimensional (2D) computer simulations of the n^+pn^+ emitter-wrap-through (EWT) cell structure with industrially relevant parameters is performed and a comparison is made with p-type substrate interdigitated back contact (IBC) cells. Our simulation results show that the EWT cell is particularly suited for low bulk lifetimes and thin substrates. Simulation results indicate that achieving a lifetime of around 45 μs will be sufficient to realize very high-efficiency EWT cells. The effect of different cell parameters (e.g., surface recombination velocities, thickness, bulk resistivity, bulk lifetime, cell geometry, etc.) is explored. The EWT cell shows much higher robustness to poor material lifetime as well as surface passivation compared to the IBC cell. While a 1 ms lifetime IBC cell drops to efficiencies less than 14.5% for an intrinsic surface recombination velocity (SRV) of 10,000 cm/s, the EWT cell can maintain efficiencies above 15% at a much lower bulk lifetime of 30 μs and higher SRV of 300,000 cm/s.

INTRODUCTION

Back-contact cells offer several advantages compared to conventional solar cells. These advantages include the elimination of grid shadowing, improved aesthetics, and simplification of cell interconnection leading to a lower module assembly cost. The EWT cell is a very promising back-contact cell for both high-efficiency and industrial feasibility [1, 2]. EWT cells give a higher current collection for lower lifetime thinner substrates since minority carriers are collected from both the front- and back-surface sides of the bulk compared to IBC solar cells. Simulation of low-cost EWT cells is critical for better understanding the physical behavior of these cells and for the optimization of the cell design and fabrication process for maximum cell performance. Our baseline low-cost EWT cell fabrication process involves high-throughput screen printing and laser drilling.

In this work, we investigate industrially relevant parameters and their effect on the EWT device performance using 2D-simulation. The effect of bulk lifetime, contact diffusions, front and back recombination velocity (FSRV and BSRV), different emitter diffusion profiles and surface fields on low-cost p-type EWT cells performance is explored. Simulation results for the EWT solar cell are compared with the IBC counterpart as well.

EXPERIMENTAL AND DEVICE SIMULATION

The substrate of our EWT cells is 1.15 Ω-cm p-type multicrystalline-Si (mc-Si). These cells are fabricated by laser drilling a 2 mm x 0.5 mm via pattern grid; the holes are about 65 μm in diameter. The starting wafers are 280-μm thick; however, they are etched and cleaned to ~260 μm thickness. The via pattern lines have a 2 mm pitch while the n and p regions have a 1 mm pitch which is shown in the modeled unit cell of Fig. 1. Our EWT process development has been described by P. Hacke et al. [3].

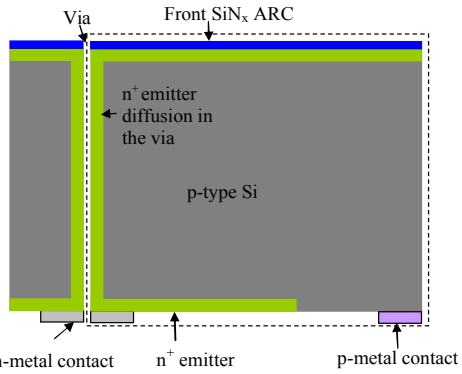

Fig. 1. Schematic of the EWT unit cell (dashed box) used in the simulation.

The 2D-simulations were performed with Microtec 4.2, a device simulation program produced by Siborg Systems, Inc. The structure of the unit cell that was used in the simulation is illustrated in Fig. 1. This paper is divided into two parts. The first part investigates Advent Solar's EWT solar cell for different physical parameters; the second part is a comparison between EWT and IBC cells with high-efficiency parameters. Our simulation uses the AM1.5D, 100 mW/cm^2 spectrum. The simulation program does not include extrinsic sources of series resistance outside the simulation domain (e.g., grid resistance), nor allow for inclusion of sources of excess recombination current (e.g., shunt resistance or junction leakage current).

RESULTS AND DISCUSSION

First we started by simulating our baseline non-textured EWT cell. The EWT cells are fabricated in a pilot production line using only high-throughput processes like screen printing, in-line PECVD, and laser drilling. Table 1 shows the I-V parameters for a 156.25 cm^2 cell fabricated at Advent Solar as well as the simulation results. The cell

Table 1. Experimental and simulated I-V parameters of the EWT cell. The FF used for the simulation results is actually assumed based on a resistance model for the EWT cell.

	J_{sc} (mA/cm^2)	V_{oc} (mV)	FF	Efficiency (%)
Experimental	35.453	598.8	71.19	15.11
Simulation	35.569	603.7	72.00	15.46

was simulated with a 10 μs bulk lifetime. The simulated short-circuit current (J_{sc}) and open-circuit voltage (V_{oc}) values are quite close to the experimental results. The ~5 mV difference in V_{oc} between the experimental and simulation can be explained by the presence of impurities in the n^+-p depletion region, which result in a junction leakage current; this is not accounted for in the simulation.

Distribution of Shockley-Read-Hall (SRH) recombination at J_{sc} illustrates the current-collection advantage of EWT cells (Fig. 2). The SRH recombination rate is higher over the p-contact region compared with the n^+ diffusion

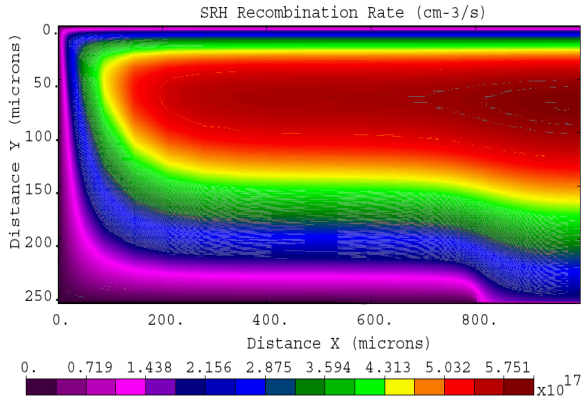

Fig. 2. SRH recombination rate (1/(cm^3.s)) at J_{sc} condition for our baseline EWT cell structure.

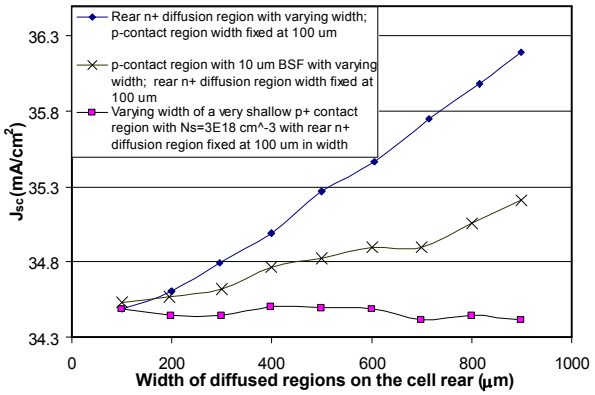

Fig. 3. J_{sc} as a function of n^+ or p^+ diffusion width on the cell rear.

region due to the current collection from the rear-n^+ diffusion. Hence, increasing the area of the rear n^+ diffusion region significantly improves J_{sc} (Fig. 3). This effect was found to be more beneficial than that of the non-diffused rear surface, the p-contact region, or a well-passivated p-contact using a back-surface field (BSF) (Fig. 3). We did not observe a significant change in either V_{oc} or J_{sc} due to a change in the n-p pitch, although the n-p pitch is a critical design parameter in more complete series-resistance models.

V_{oc} is dominated by recombination in the n^+ emitters and the bulk – while the recombination in the via surface and p-type surfaces were found to be less significant. This indicates that the FSRV and bulk lifetime in the current pilot production process are limiting cell performance. The recombination at the p-type surfaces (BSRV of the non-diffused surface and at the p-type contact region) become more significant at higher bulk lifetime because of the longer minority-carrier diffusion length (L_{bulk}) (Fig. 4).

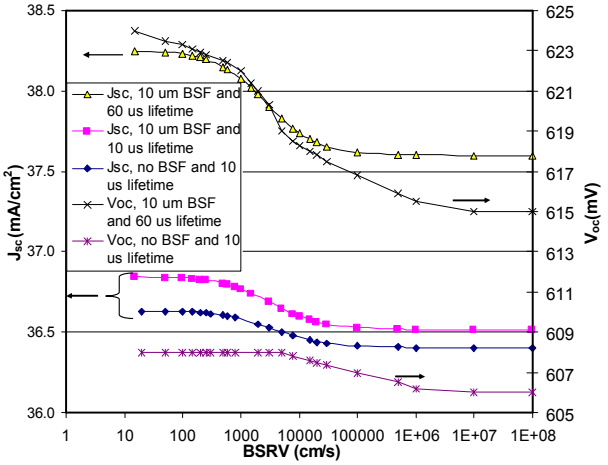

Figure 4. J_{sc} and V_{oc} as a function of BSRV (in between the n- and p-ohmic contacts) for lower and higher lifetime with and without a BSF. FSRV is set at 30,000 cm/s.

Nevertheless, the effect of BSRV on J_{sc} is still smaller than that of FSRV (Fig. 5) even for higher lifetime substrates. The V_{oc} change with BSRV is also increased significantly

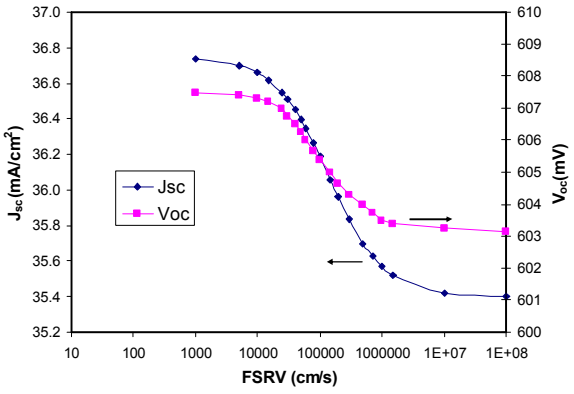

Fig. 5. J_{sc} and V_{oc} of the EWT cell as a function of FSRV. BSRV (in between rear contacts) is set at 1×10^7 cm/s and a 10 μs lifetime is used.

for the higher bulk lifetime. Kress et al. have previously shown using two-dimensional computer modeling that the surface recombination velocity in between the neighboring n and p contacts strongly affects the open-circuit voltage

[4]. The front-surface diffusion profile determines how strong of an effect the FSRV has on J_{sc}; for example, a driven diffusion with surface concentration (N_s) of 5×10^{18} cm^{-3} will yield a J_{sc} of ~27.7 mA/cm^2 for a very high FSRV (1×10^6 cm/s) while a shallow diffusion with $N_s=2.5\times10^{20}$ cm^{-3} will yield a J_{sc} of ~35.5 mA/cm^2 for the same high FSRV. Figure 6 shows that the V_{oc} increases with a deeper diffusion underneath the n-metal ohmic contact. This is due to the mitigation of the surface recombination underneath the n-metal contact.

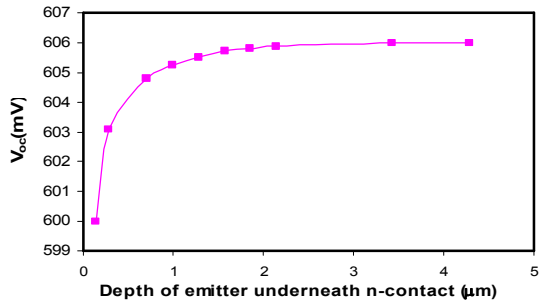

Fig. 6. V_{oc} as a function of EWT rear n^+ emitter depth.

Generally, as the bulk resistivity increases the J_{sc} increases and V_{oc} decreases. The FF, which is not modeled here, should decrease with higher base resistivity since it is dependent on the V_{oc} but also because the lower base resistivity reduces edge diode resistance over the n-busbar and n-gridlines [5]. A FF of 0.72 was assumed for the efficiency plot in Fig. 7. Lower base resistivity showed a higher efficiency with an optimum around 0.7 Ω-cm. The model includes a lifetime dependence on base resistivity.

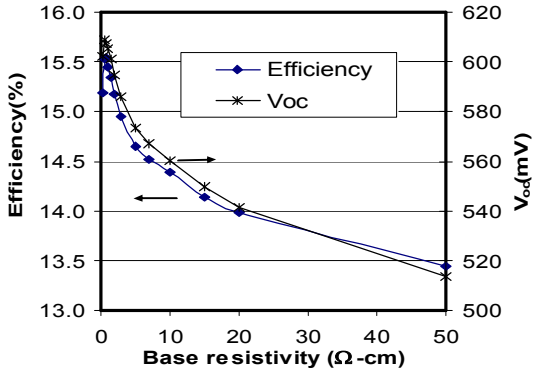

Fig. 7. Effect of base resistivity on V_{oc} and efficiency of the EWT cell.

To understand the requirements for lifetime in order to achieve high performance cells the J_{sc} and V_{oc} are plotted as a function of bulk lifetime for our baseline EWT device parameters and design. As shown in Fig. 8, the V_{oc} and J_{sc} reach a saturation point at around 45 μs where the performance reaches a plateau. This is also true for an improved surface recombination velocity (SRV) of 30,000 cm/s. This is not the case for a conventional solar cell where the V_{oc} continues to increase with higher bulk lifetime (Fig. 8).

Since there is a strong interest in using thinner Si wafers to reduce the cost of Si material, and hence, the overall cost of the PV module, simulations of EWT cells with different thicknesses (W) and lifetimes were performed. As shown in Fig. 9, for low lifetimes (similar to

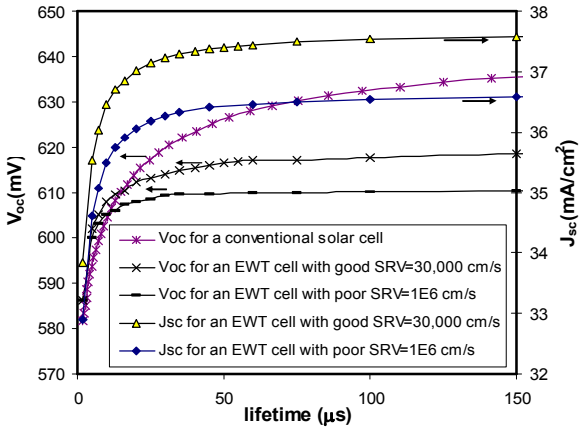

Fig. 8. V_{oc} and J_{sc} as a function of minority-carrier lifetime for different front- and back-surface recombination velocities.

those of as-grown mc-Si) the EWT cell maintains a high efficiency with a broad peak for thinner substrates (~100 μm). This peak shifts to thicker substrates as we go to higher lifetimes (Fig. 9). For the low bulk lifetimes (<10 μs), the V_{oc} is highest for the thinner substrates of 100 μm

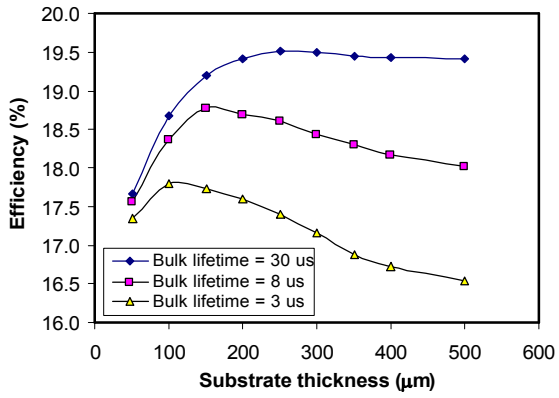

Fig. 9. Efficiency of the EWT cell as a function of substrate thickness for different minority-carrier lifetimes (τ_b). An SRV=30,000 cm/s is used in the simulations and a FF=0.72 is assumed.

cell thickness, due to a reduction in the bulk recombination component with thickness. For the 30 μs bulk lifetime the V_{oc} is highest for a 150 μm cell thickness. The results also show that for low minority-carrier lifetime material the efficiency peaks at a thickness about two times the minority-carrier diffusion length ($W=2L_{bulk}$). This indicates that the EWT structure works particularly well for low-lifetime thin substrate cells. Thin substrates should also improve the FF due to the decrease in the hole resistance.

The effect of rear dielectric fixed surface charge density (Q_f) was also simulated for our EWT cell (Fig. 10).

In our baseline cell we have a diffusion barrier that separates the n^+ and p-contact regions, however, if we were to remove it and have a SiN_x film in its place, fixed positive charge would be present at the rear surface in between the n and p ohmic contacts. As illustrated in Fig. 10 higher positive charge density initially reduces the V_{oc} due to formation of a depletion region at the surface; the

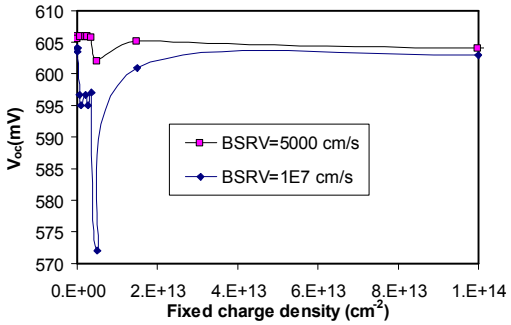

Fig. 10. V_{oc} as a function of Q_f of a rear dielectric between the n and p ohmic contacts.

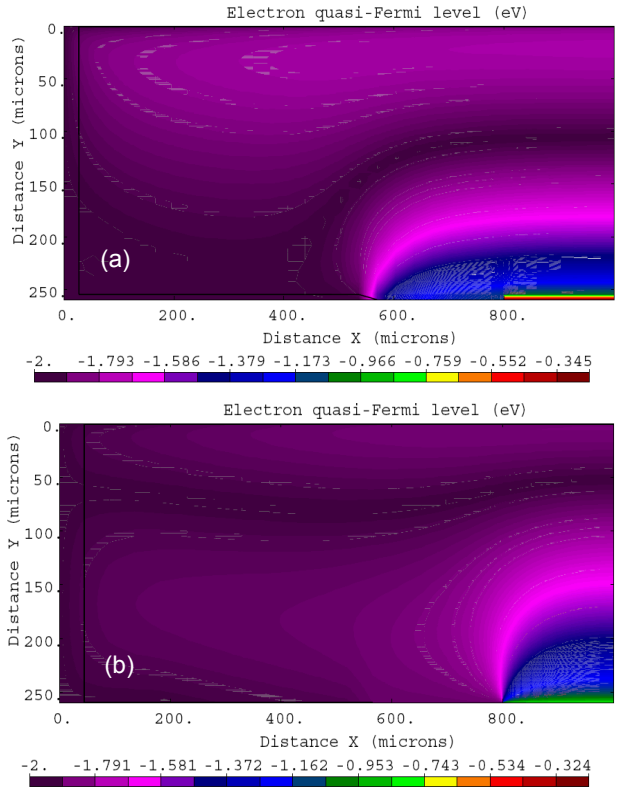

Fig. 11. Electron quasi-Fermi levels (log(eV)) for an EWT cell simulated with Q_f of (a) 5×10^{12} cm^{-2} and (b) 1×10^{14} cm^{-2} on the rear side in between the n- and p-ohmic contacts.

depletion region increases recombination due to the electric field aiding electron current flow. However, increasing Q_f to 1×10^{14} cm^{-2} and above improves V_{oc} due to the formation of an inversion layer. The inversion layer is evident in the plot of the quasi-Fermi levels (Fig. 11). The floating junction (due to the inversion layer) becomes an extension of the n^+ diffusion region on the rear, but might also be a source of shunt current that is not adequately modeled in the simulation [6]. Having a low SRV in between the n and p contacts significantly reduces the loss in V_{oc} due to the charge-induced depletion region recombination (Fig. 10).

In the remaining part of this paper we compare the performance of the IBC cell with the EWT cell for high-efficiency implementation. The geometry of the modeled IBC cell is the same as its EWT counterpart except that there is no left side diffusion in the unit cell shown in Fig. 1. The base resistivity (1.15 Ω-cm) and diffusion profiles used for the simulation of both devices are also the same. The efficiency in the following plots is calculated for a FF of 0.79 in case of the IBC cell and 0.775 for the EWT cell. The lower FF assumed for the EWT cell is to account for the hole resistance. However, the hole resistance as well as the current crowding into the via openings could be made negligible by having a heavily doped n+ emitter in the holes and around the openings. The IBC and EWT cells were also modeled with an excellent back reflectance and low front reflection (for a textured surface). Figure 12 shows that the EWT cell reaches a plateau for higher efficiencies at an earlier bulk lifetime (~60 μs) compared with the IBC cell, which shows a plateau in efficiency

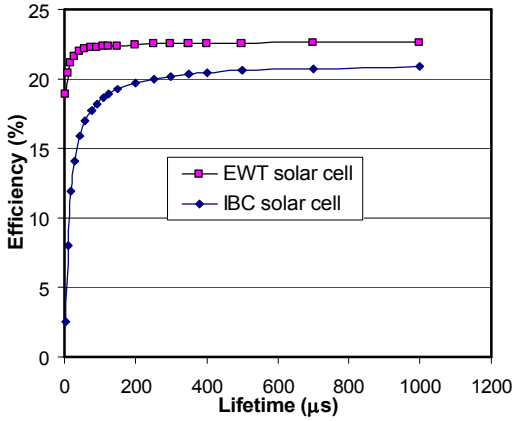

Figure 12. Efficiency as a function of minority-carrier lifetime for the IBC and EWT cells. An SRV of 500 cm/s is assumed for both cases.

starting at ~250 μs. Our results are in agreement with previous work comparing the EWT and IBC or rear-contacted cells [7-9], which found that the EWT cell can yield high J_{sc} and high efficiency even for substrate material diffusion lengths less than the cell thickness. As shown in Fig. 13, the difference between the EWT and IBC solar cell is very significant as the EWT cell can achieve efficiencies >20% with $W=2.5L_{bulk}$. The EWT cell maintains higher efficiencies at higher SRVs that are still quite good by the photovoltaic industry standards compared with very poor performance for the IBC cell (Fig. 13). For example, at ~10,000 cm/s (lower FSRV values are possible for a low N_s emitter) the performance of the IBC cell is already comparable to industrial front-contact conventional solar cells, while the EWT cell achieves high efficiencies ~19%. Moreover, the EWT cell

was modeled with a 30 μs lifetime as opposed to 1 ms for the IBC cell.

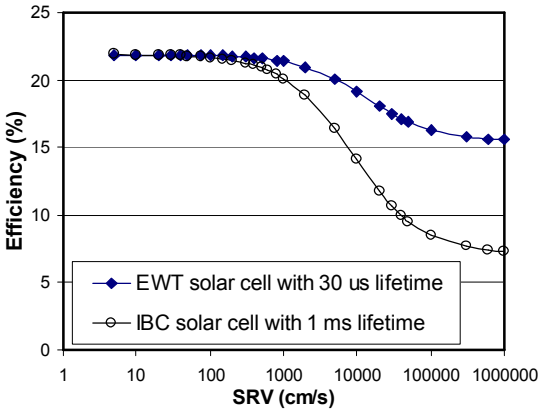

Fig. 13. Efficiency as a function of FSRV and BSRV for the IBC and EWT cells. A 12-μm deep BSF is assumed for both devices.

Consistent with the above results, the EWT cell appears to be less sensitive to a BSF compared with the IBC cell for the same bulk lifetime (60 μs) as shown in Fig. 14. This is because in the case of the IBC cell, it is easier for more minority carriers (electrons) to recombine at the p-contact before being collected at the n^+-p junction. In the case where there is no BSF there is a significant drop in J_{sc} for the IBC cell, which is much lower (~34 mA/cm^2) compared with the J_{sc} of the EWT cell with no BSF, which

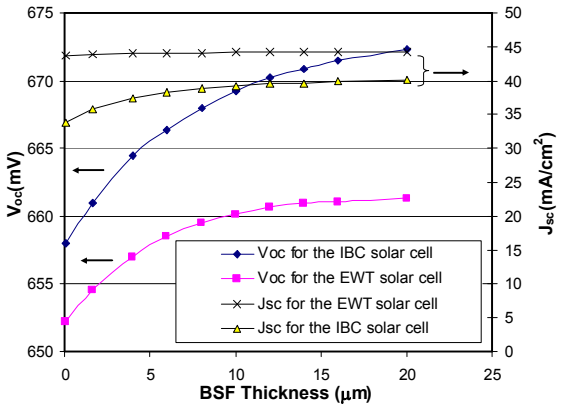

Fig. 14. Effect of BSF thickness on V_{oc} and J_{sc} for EWT and IBC cells. A bulk lifetime of 60 μs is assumed for both devices. The BSF has a surface concentration of 3×10^{18} cm^{-3}.

remains high.

CONCLUSION

Computer simulation results indicate that achieving lifetimes >45 μs will not result in a significant gain to the EWT cell performance. Increased n^+ region for minority carrier collection significantly enhances J_{sc} and the EWT cell performance. In order to reach efficiencies of 16% or higher at low bulk lifetime the FSRV would need to be improved to <70,000 cm/s. Our modeling results demonstrate that the EWT cell is a much more robust device compared to the IBC cell. The EWT cell is less sensitive to lower bulk lifetime as well as surface recombination velocity compared to the IBC cell. These properties make the EWT cell particularly well-suited to low-cost processing as well as low-lifetime multicrystalline substrates. The EWT cell appears to be less sensitive to the effect of having a BSF compared with the IBC cell. Experimental results of our baseline EWT cell also indicate the robustness of the EWT cell performance to surface passivation as well as low bulk lifetimes. Future work should focus on improving the FSRV as well as the FF while maintaining a lifetime of around 30-45 μs.

REFERENCES

[1] J. M. Gee, W. K. Schubert, and P. A. Basore, "Emitter Wrap-Through Solar Cell," *23rd IEEE PVSC*, 1993, pp. 265-270.

[2] J. M. Gee, P. Hacke, M. W. Sumner, and R. R. Schmidt, "Towards a Manufacturable Back-contact Emitter-Wrap-Through Silicon Solar Cell," *31st IEEE PVSC,* 2005, pp. 1663-1666.

[3] P. Hacke, J. M. Gee, M. W. Sumner, J. Salami, and C. Honsberg, "Application of a Boron Source Diffusion Barrier for the Fabrication of Back Contact Silicon Solar Cells," *31st IEEE PVSC,* 2005, pp. 1181-1184.

[4] A. Kress, R. Kühn, P. Fath, G. P. Willeke, and E. Bucher, "Low-Cost Back Contact Silicon Solar Cells," *IEEE Transactions on Electron Devices*, **Vol. 46,** No. 10, 1999, pp. 2000-2004.

[5] D. D. Smith, J. M. Gee, M. D. Bode, and J. C. Jimeno, "Circuit Modeling of the Emitter-Wrap-Through Solar Cell," *IEEE Transactions on Electron Devices*, **Vol. 46**, No. 10, 1999, pp. 1993-1999.

[6] S. Dauwe, L. Mittelstädt, A. Metz, and R. Hezel, "Experimental Evidence of Parasitic Shunting in Silicon Nitride Rear Surface Passivated Solar Cells," *Progress in Photovoltaics*, **Vol. 10**, 2002, pp. 271-278.

[7] D. Kray, J. Dicker, D. Osswald, A. Leimenstoll, S.W. Glunz, W. Zimmermann, K. –H. Tentscher, and G. Strobol, "Progress in High-Efficiency Emitter-Wrap-Through Cells on Medium Quality Substrates," *WCPEC-3*, 2003.

[8] D. Kray, J. Dicker, S. Rein, F. –J. Kamerwerd, D. Oβwald, E. Schäffer, S. W. Glunz, and G. Willeke, "High-Efficiency Emitter-Wrap-Through Cells, 17th EU-PVSEC, 2001, pp.1299-1302.

[9] S. W. Glunz, J. Dicker, D. Kray, J. Y. Lee, R. Preu, E. Schneiderlöchner, J. Sölter, W. Warta, and G. Willeke, "High-Efficiency Cell Structures for Medium-Quality Silicon," 17th EU-PVSEC, 2001, pp.1287-1292.